Precision Attitude Determination of Spacecraft Using Star Trackers and Developments of Ground Test-bed

Abstract — In this paper a star pattern identification algorithm is addressed for the precision attitude determination of spacecraft. Proposed algorithm is associated in term of pattern recognition. Each star is related with well-defined pattern that can be determined by the surrounding stars. There is well-known the grid algorithm as one of the star identification algorithms related to pattern recognition. The proposed algorithm is based on the grid algorithm. Modification methods, polar grid, virtual grids and multi-references, are proposed to enhance the grid algorithm. The proposed modified grid algorithm is also demonstrated by the numerical simulation. For the ground tests of the proposed algorithm, Star pattern generation software, star identification software and a hardware system are developed.

INTRODUCTION

Whenever the mission is voyaging into the deep space or orbiting the earth, the spacecraft must have accurate guidance information. Reliable guidance information enables the spacecraft to achieve the given mission reliably. Especially, the loss of the guidance control information during a voyage is big potential threat. Obtaining the guidance information is addressed in this paper establishing an attitude determination algorithm using star patterns.

The efficient identification technique called grid algorithm has been introduced to overcome the disadvantage of conventional angle matching method[6]. The grid algorithm is classified as pattern recognition. The algorithm has a database in which each star has well defined pattern determined by the surrounding stars in the specified field of view. Measured star field by the star tracker is converted a specified pattern by various methods. The pattern can be identified by finding the best matching pattern in the star pattern database. The grid algorithm is known to be robust with respect to sensor noise. It also requires less computer resources compared to other algorithms because of its simplicity.

A modified grid algorithm for more accurate and reliable identification is introduced. A promising star identification approach proposed in this paper is to use multi-reference stars with which specific patterns are to be identified. If there is noise in the CCD(Charge Coupled Device) image detector, a single reference star could be mis-identified with the generated grid database. However, the possibility of mis-identification can be reduced for the final star identification by selecting the multi-reference stars as addressed in this study. Another useful proposed approach is to generate *virtual grids*. The reference stars outside of the pattern radius are always eliminated in the original grid algorithm since they are located far from the selected reference star. This may lead to mis-identification by eliminating the reference stars because since they could

provide useful information. The reference stars eliminated in the original algorithm are employed in this study by the grids generated virtually on the outside of the virtual CCD plane. The virtual grid covers the area beyond that defined by the pattern radius in the original grid algorithm.

The best way to test the star trackers is to use the CCD star images captured in the real sky. However, obtaining the images is very limited due to the error sources of the atmosphere. In this paper, a ground-based test system is developed to overcome the problem. This system consists of three parts: one is pattern generation software, another is star pattern identification software, and the last one is the overall hardware system.

General grid algorithm is first introduced briefly in this study. Then the modified methods are applied to the original grid algorithm for performance enhancement. Simulation studies include how many reference stars and how many virtual grids are effective for star identification. Thus a guideline for selecting suitable parameters for efficient identification is established. Also, star identification probability versus position accuracy of the image in the CCD plane is presented. The simulation results show that it is more stable about the Gaussian noise in the CCD image detector compared to the original grid algorithm. Obviously, the grid algorithm is generally known to be robust compared to general angle matching technique[6]. The modified grid algorithm proposed in this study provides robust star identification performance over a wide range of sensor noise. To demonstrate the proposed algorithm within actual environment a ground test system is introduced and a ground test is performed.

GRID ALGORITHM

The grid algorithm is a pattern recognition algorithm for star field detected on the CCD plane of the star tracker. The main idea of the algorithm is to generate a specified pattern database and to construct a grid pattern from the measured star field on the CCD plane. The specific grid pattern is first generated using the grid. As searching the pattern database already designed by the grid algorithm, the specific pattern can be identified as an identified star. In this section, we introduce the grid algorithm.

A set constituted by the stars in the specified field of view is needed to be pattern. Each star in the set is called *reference star*. The pattern is constructed in the following manner [6]. First, on select a reference star, *pivot star*, in the set. The pivot star is the star to be identified by the given database. And then, part the sky of the surrounding sky within *pattern radius* (r_p) which center is pivot star position. The pattern radius can be determined by function of the FOV(Field Of View) and a marginal value. Thus, translate the pivot star in the center of the FOV and related reference stars also translate with same length with pivot star. And then, one can select a closest reference star, *alignment star*, whose distance to the pivot star is marginally bigger than the *buffer radius* (r_b). Then, orient the alignment star to the reference frame so that the related reference stars rotate with the same angle. Finally make a grid of size $g \times g$ in the pattern. If a grid cell contains a reference star, let the cell be 1 otherwise 0 to generate a standard format for the pattern. Bits of the grid cell are pattern information of each star in the real sky. The database is constituted by the bits information about each star.

After the pattern is constructed, we must determine which pattern in the database is related closely with the imaged pattern on the CCD plane of the star tracker. The imaged pattern can also be generated a standard format by using same manner in the previous paragraph. If there are many shared or matched cells between the imaged pattern and a pattern in the database, it could be a candidate star to be identified. When there is only one candidate star, the candidate star can be treated as the matched star. However, if there are a lot of candidate stars through the cell matching process, the candidate star of containing the maximum matching cells is assumed as the identified star.

Database Generation

The method of generating a set of patterns which constitute a database is introduced. The reference stars are known beforehand from a star catalog bright star catalog (BSC) is used in this paper. BSC contains star brightness, right ascension and declination with respect to the inertial frame. There are 9110 stars. The coordinate of the star is defined in Fig.1.

We introduce some useful notation as shown Fig.1. $\mathbf{s}$ denotes the unit star vector in the real sky with respect to the inertial frame. $\mathbf{s}_p$ is a pivot star vector. And $\mathbf{p}$ is the star vector imaged on the CCD plane

with respect to the CCD body frame. The length of the $\mathbf{p}$ is defined and related with the focal length(f). $\mathbf{p}_r$ is a pivot star vector imaged on the CCD with its length identical to the focal length

$$|\mathbf{p}_r| = f \tag{1}$$

θ_i is the angle between pivot star and ith reference star. The length of the $\mathbf{p}_i$ is then given as

$$|\mathbf{p}_i| = \frac{|\mathbf{p}_r|}{\cos\theta_i} \tag{2}$$

An imaged star vector ($\bar{\mathbf{p}}_i$) attached on the CCD plane can be expressed as

$$\bar{\mathbf{p}}_i = \mathbf{p}_i - \mathbf{p}_r \tag{3}$$

The x value of the imaged star vector is 0 with respect to the CCD body frame. φ is the right ascension and ς is the declination with respect to the inertial frame.

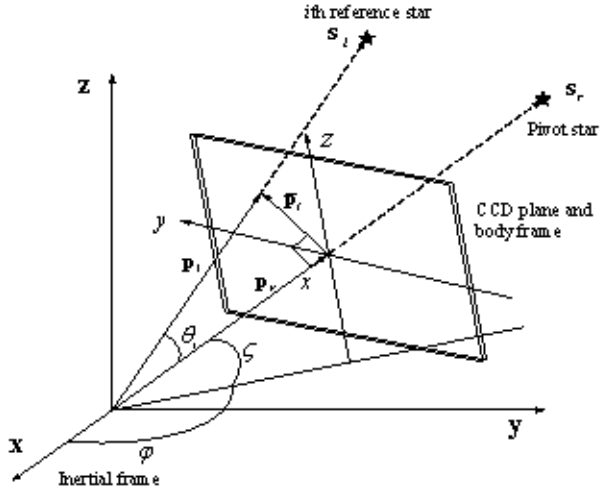

Fig.1 Definition of the inertial frame and CCD body frame.

From the geometric relations shown in Fig.1, the star vector ($\mathbf{s}$) is given as

$$\mathbf{s} = \begin{bmatrix} \cos\varsigma\cos\varphi & \cos\varsigma\sin\varphi & \sin\varsigma \end{bmatrix}^T \tag{4}$$

The direction cosine matrix to CCD body frame from inertial frame is given as

$$C_I^B = \begin{bmatrix} \cos\varphi\cos\varsigma & -\sin\varphi\cos\varsigma & \sin\varsigma \\ \sin\varphi & \cos\varphi & 0 \\ -\cos\varphi\sin\varsigma & -\sin\varphi\sin\varsigma & \cos\varsigma \end{bmatrix} \tag{5}$$

where we used $C_3(\varphi) \rightarrow C_2(-\varsigma)$ rotational sequence.

To obtain a set constituted by the stars in the specified field of view using the catalog information, every stars in the catalog can be transformed such as Eqn.(4). The set with a pivot star is limited by a threshold angle. Thus, the related reference stars in the set are simply chosen by the inner product relationship such as

$$\theta_i = \cos^{-1}(\langle s_i, s_r \rangle) < \theta_t \tag{6}$$

where θ_t is a threshold angle. $\langle , \rangle$ denotes a vector inner product. The threshold angle which is closely related with the pattern radius given by

$$\theta_t \geq \tan^{-1}(r_p / f) \tag{7}$$

Thus, one can obtain reference stars which have smaller angle between the reference star and pivot star than the threshold angle.

Since we must know the position in the CCD plane for grid pattern generation, the star vector ($\mathbf{s}$) in the real sky can be transformed by the direction cosine matrix in the

$$\mathbf{p}_i = | \mathbf{p}_i | C_I^B \mathbf{s}_i \tag{8}$$

where the body frame is defined in Fig.1. Inserting the Eqns. (1)-(2) and (6) into the Eqn.(8), we can obtain the imaged star vector in the CCD plane as

$$\mathbf{p}_i = \frac{f}{\langle s_i, s_r \rangle} C_I^B \mathbf{s}_i \tag{9}$$

The Eqn.(9) means that the ith star ($\mathbf{s}_i$) in the real sky with respect to the inertial frame is transformed to an imaged star vector in the CCD body frame. Moreover, 2D star vector in the CCD plane denotes just $\hat{\mathbf{p}}_i = (-y, z)$ for convenience.

The rotation process should be achieved to make a standard format based on grids. To select a align vector which is the closest reference star outside the buffer radius, one can define a error equation given by

$$e_i = | \hat{\mathbf{p}}_i | - r_b \tag{10}$$

thus, a align vector can be determined by

$$\min_i (e_i) \quad \text{and} \quad e_i \rangle 0 \tag{11}$$

One can rotate the align vector to be aligned with $-y$ axis in the CCD body frame also obtain the rotational angle. All the neighboring stars in the set are also rotated with the same angle. Now we have a well-defined pattern through the orientation process.

To formulate a sensor pattern vector which is constituted by the cell indices, The CCD plane must be

divided by the grid. We assume that the star tracker has a CCD plane of size $m \times m$ and grid of size $g \times g$ shown in Fig.2. The cell index starts on the bottom of the left side and increases by moving to the right direction and also to the upper direction.

Thus, to obtain the relationship between the neighboring star position and cell index, we can make $\hat{\mathbf{p}}_i$ be an integer as,

$$\begin{aligned} \overline{x}_i &= \mathrm{int}\left(\frac{2x_i' + m}{2m} g\right) + 1 \\ \overline{y}_i &= \mathrm{int}\left(\frac{2y_i' + m}{2m} g\right) + 1 \end{aligned} \tag{12}$$

The pair $(\overline{x}, \overline{y})$ can be expressed by a function of pattern radius(r_p), since the pattern radius is associated with the CCD size given as

$$r_p = m/2 \tag{13}$$

The cell indices of the ith neighboring stars about pivot star $(\mathbf{p}_r)$ can be expressed as

$$c_{ki}(\overline{x}_i, \overline{y}_i) = (\overline{y}_i - 1) g + \overline{x}_i \tag{14}$$

Assume that the kth star in the star catalog by a pivot star has bases of number of h_k, the database constituted the imaged star vectors for grid algorithm can be expressed Table I.

Table I. Database configuration.

Star index	Total cells	Imaged star vector
1	h_1	$c_{11}, c_{12}, c_{13} \ldots c_{1h_1}$
2	h_2	$c_{21}, c_{22}, c_{23} \ldots c_{1h_2}$
….		…
n	h_n	$c_{n1}, c_{n2}, c_{n3} \ldots c_{1h_n}$

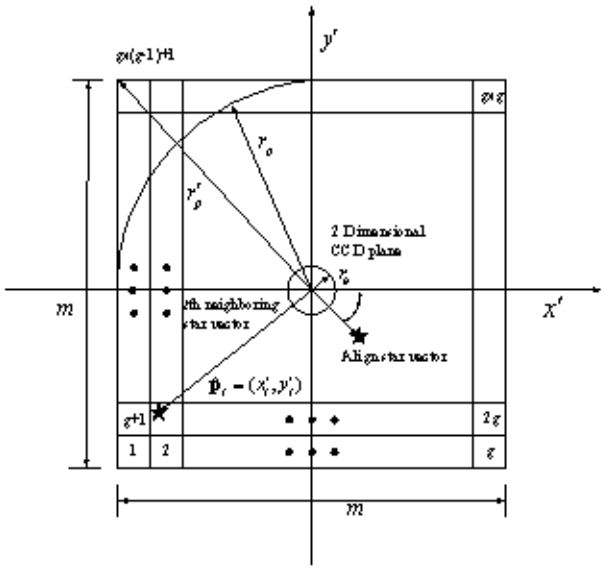

Fig.2 Grid pattern and CCD plane configuration.

Pattern Generation from CCD Plane

From the CCD plane of the star tracker, we can obtain an actual image of the star field. The imaged pattern can also be converting a standard format. Only one thing to do in the process is to relocate a selected pivot star ($\mathbf{p}_r$) to the center and neighboring stars also to be relocated in the CCD image. This process can easily be obtained by the rotational sequence. To reduce the computational burden, we can assume that the pivot star is close to the center. The process is constructed by Euler rotation sequence that the angles (α, β) between x axis vector of the body frame and the pivot vector. Since the angles are assumed small, it can be approximately obtained from the pivot star location with respect to the body frame as $\mathbf{p}_r \approx (f, \alpha, \beta)$.

The imaged star ($\mathbf{p}_i$) on the CCD plane of the star tracker with body frame coordinated system can be approximately relocated such as

$$\mathbf{p}_i' \approx f \frac{|\mathbf{p}_r|}{\langle \mathbf{p}_i, \mathbf{p}_r \rangle} \begin{bmatrix} 1 & -\alpha & \beta \\ \alpha & 1 & 0 \\ -\beta & 0 & 1 \end{bmatrix} \mathbf{p}_i \tag{15}$$

where $C_3(\alpha) \rightarrow C_2(-\beta)$ rotational sequence is used.

MODIFICATION METHODS

The grid algorithm introduced in the previous section is known to be an autonomous and reliable algorithm. To identify the given image and to eliminate any ambiguity, at least two stars are required. However, for more reliable identification, over 10 stars are should be measured on the CCD. If there is noise on the CCD so that a wrong alignment vector is chosen, its orientation may be different from that of the database. This may be a critical problem to star pattern identification.

In this section, we introduce some useful methods to enhance the grid algorithm. The first is to use polar coordinate grid shown in Fig.4 instead of the Cartesian grid (original grid algorithm).As mentioned in the previous section, the measured pattern is relocated and orientated by the pivot star to make the standard format. Even if the position of the pivot star is perturbed by the CCD noise or other factors, the relocated amounts of the neighboring stars also have same errors with that of the pivot star has. This error is inevitable. However, the orientation process is different. If the position of the selected align vector has some position error, close neighboring stars with the pivot star have much same errors. But the reference stars far from the pivot star have much errors linearly proportional to the length of the reference stars given by $r_i\varepsilon$ where ε is angle error of the align vector. This result is shown in Fig.3

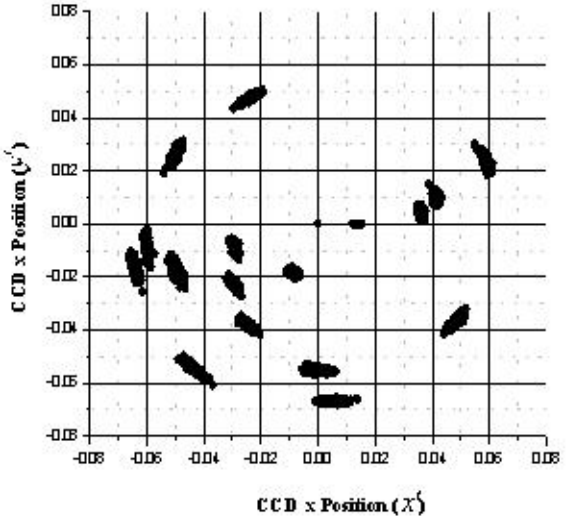

Fig.3 Pattern errors due to the position errors

These position errors may be occurred by the CCD array resolution limit and photo shot noise also can be

a critical source of the noise. To reduce the position error due to the rotational process, we design a polar cell whose residual space to the angular direction has more margins as shown in Fig.4.

There can be various methods to make grid index sequence in the case of polar coordinated system. Using normalized radius, the length difference between the outer and inner neighboring circle is 2π. One method proposed in this paper is to list the grid index.

To make polar a grid size of g_θ per 2π about non-dimensional unit radius and also the non-dimensional radius (integer) up to g_r, the grid index of the ith reference star about kth star in the star catalog can be written as

$$c_{ki}(\bar{r}_i, \lambda_i) = \mathrm{int}\left\{\frac{g_\lambda \bar{r}_i(\bar{r}_i+1)}{2}+1\right\} + \mathrm{int}\left\{\frac{\lambda_i}{2\pi} g_\lambda (\bar{r}_i+1)\right\} \tag{16}$$

where the non-dimensionalized radius is expressed as

$$\bar{r}_i = \mathrm{int}\left(\frac{r_i}{r'_p} g_r\right) \tag{17}$$

The ith reference star is denoted as $\hat{\mathbf{p}}_i = (r_i, \lambda_i)$.

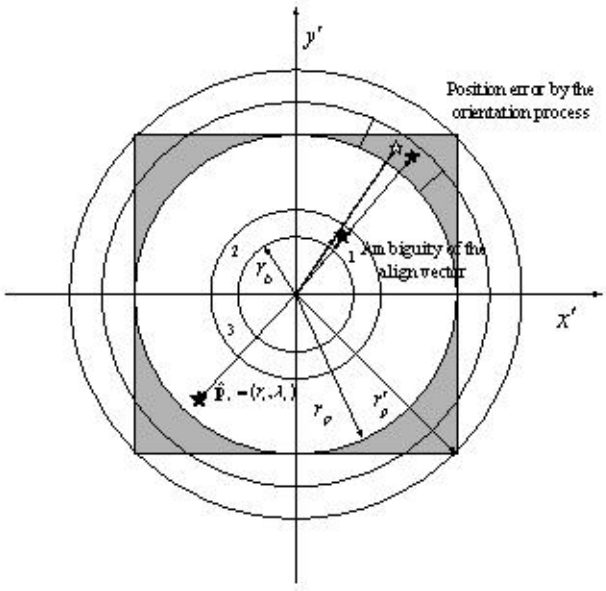

Fig.4 Polar coordinated grid pattern

The standard format of the Cartesian grid is based on the area of the given CCD plane. The pattern radius

in the original coordinated grid is the same as half of the CCD plane width. When the pivot star is relocated to the center of the CCD plane, the reference stars outside of the pattern radius cannot be expressed properly. Even if a reference star that may be a critical star in identifying the pattern is located outside of the buffer radius, it is eliminated by the limit of the buffer radius. The area is shown in Fig.4 by gray color. To use the reference star outside of the pattern radius, the pattern radius should have a larger value than the length of the half of the CCD plane width.

At this point, we propose *virtual grid* which can be generated outside of the CCD plane. The virtual grid is also shown outside of the CCD plane in Fig.4. To use the virtual grid, the database is regenerated by replacing the pattern radius. In this process, more reference stars can be included in the database. It is obvious that size of the database is larger than that with smaller pattern radius. For more reliable autonomous system for star identification, it is inevitable that the database size is bigger by due to increased the pattern radius.

Finally we propose a *multi-pivot selection* algorithm to identify the captured star under the system noise. The proposed method is emphasized when the high level of noise is incorporated in the CCD image. The position accuracy is degraded by the spuriously added or lost stars which may happen in the clustering process to make a star from the charged pixels. The neighboring pixels which includes these undesirably or spuriously charged pixels are clustered as a reference star. In the clustering process, the unwanted pixels have a bad influence determining the accurate position of the clustered pixels. When these factors - spurious stars and position error - are interfaced with the alignment vector and pivot vector, it could cause a serious problem. The influence of the position error of the alignment vector could be covered partially by using the polar coordinated grid mentioned in the previous section, even if the position error of the pivot vector is inevitable. However, when a spurious star is treated as pivot star or alignment vector, grid algorithm may fail.

The proposed multi-pivot selection strategy may be applied to enhance the reliability of the grid algorithm. When a not-existing star is selected as a pivot vector or an alignment vector by the CCD noise, there are less or no matching reference stars within the database. The best matching star may not guarantee the minimum threshold value required to be a candidate star. In this case, one can select another reference stars as the pivot star and alignment vector apart from the already selected star. The newly selected stars must be located as far as possible so that the previously selected stars can be excluded from selection as the alignment vector. If the position difference between first pivot star and second pivot star is allowable for the given threshold, one can be assure that the best matching star be an identified star. If it is not allowable, we can assure that the star identification algorithm is fail. However, we can get accurate information from the multi-pivot selection strategy without mis-identification.

SIMULATIONS

A numerical simulation is performed to verify the proposed algorithm. The proposed algorithm is compared to the original grid algorithm on same conditions. For simulation, we used BSC. The stellar magnitudes range down to 8.0th level. The star tracker configuration for the simulation uses an 8×8 degree FOV with an image plane consisting of 512×512 pixels. Also the sensitivity of the star tracker assumed about 8.0 units apparent stellar magnitude. We basically are assumed that all stars in the catalog can be detected by the star tracker. However, for more reasonable simulations, Gaussian noise with standard deviation of 0.4 unit apparent stellar magnitude is added so that some stars may be not detected by the CCD plane.

The pattern radius is selected as 4 degrees which is the half of the FOV and the buffer radius is designed as 10 pixels. The grid algorithm make use of a 20×20 grid. For the polar coordinated grid algorithm, pattern radius is also designed as 4 degrees and $g_\lambda = 4, g_r = 20$. This design value is very favorable with the Cartesian grid. All of the stars in the BSC are used to generate the grid databases. The number of the reference stars near a selected pivot star is plotted in Fig.5. Some pivot stars have much less reference stars that it may be impossible to identify it. There are more about 10 reference stars which are reasonable numbers to be identified.

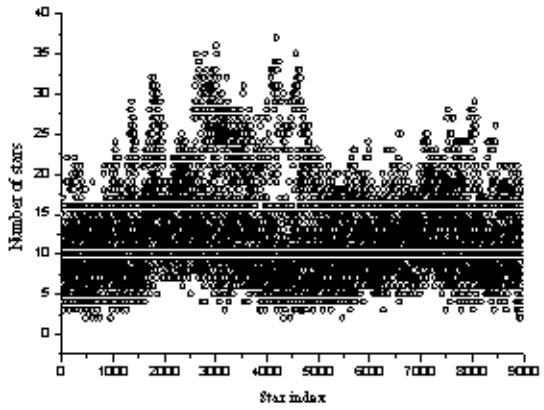

Fig.5 Number of Reference stars near the pivot stars in the 8×8 FOV.

To analyze the performance of the grid algorithm, we have added some position errors which were generated by random Gaussian noise. It has a wide range of position noise covering 0~4 pixels. The probability of the cells identified as same cells versus the position errors of the reference stars in the virtually

generated CCD plane is shown in Fig. 6. As the position error increases, one can see that the probability decreases. We can also conclude by the simulation result that the polar coordinated grid algorithm is more autonomous for the position errors than the Cartesian grid. This is because the angular direction errors are increased by the position of the radial direction. The polar coordinated grid could be made more autonomous for this error factor by properly increasing the width of the cell in the angular direction.

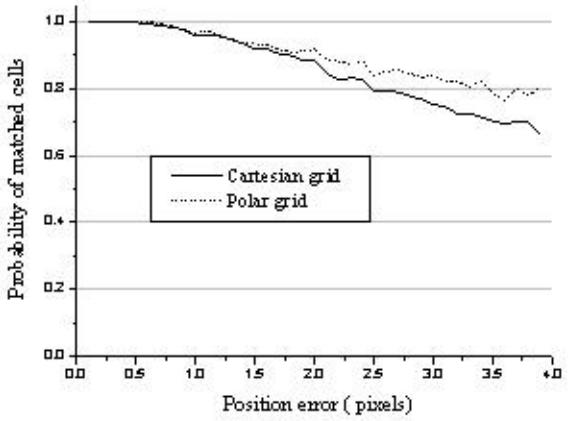

Fig.6 Probability of matched cells versus position errors of the reference stars

The probability of star identifications is shown in Fig.7. This result is generated with 1000 randomly selected bore sight of the star tracker at each position errors. The probability of the polar grid algorithm is somewhat better than the Cartesian grid. The polar coordinated grid and the Cartesian grid are compared in Fig.8. This result is based on 1.5 pixels position error. Linearly increasing right ascension, and randomly selected declination bore sight is simulated. From the results shown in Fig.8, one can easily understand the identification performance. The difference matched cells is viewed in the last figure in Fig.8. Polar grid algorithm has more cells to be matched correctly about 1.5 times many cells.

For navigation purposes, the probability of star identifications shown in Fig.7 is less confidential. The less reference stars captured in the image about randomly generated bore sight also spuriously matched stars cause this result. To enhance the performance of the algorithm, proposed methods in this paper are applied to the previous simulation results in Fig.7. Simulation result applied proposed virtual grid is shown in Fig. 9. The proposed virtual grid is very distinguishably enhancing the grid algorithm. Both the polar grid algorithm and Cartesian grid algorithm show enhanced star identification probability when using the virtual grid

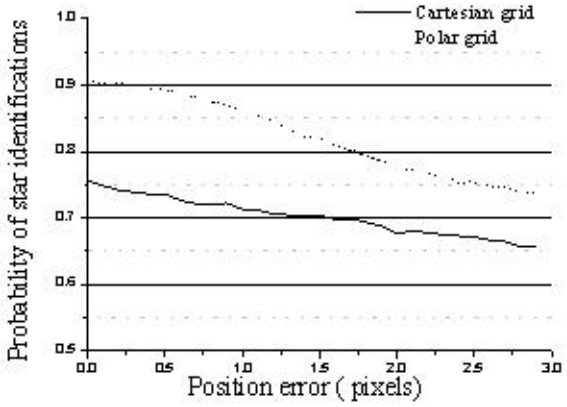

Fig.7 Probability of star identification

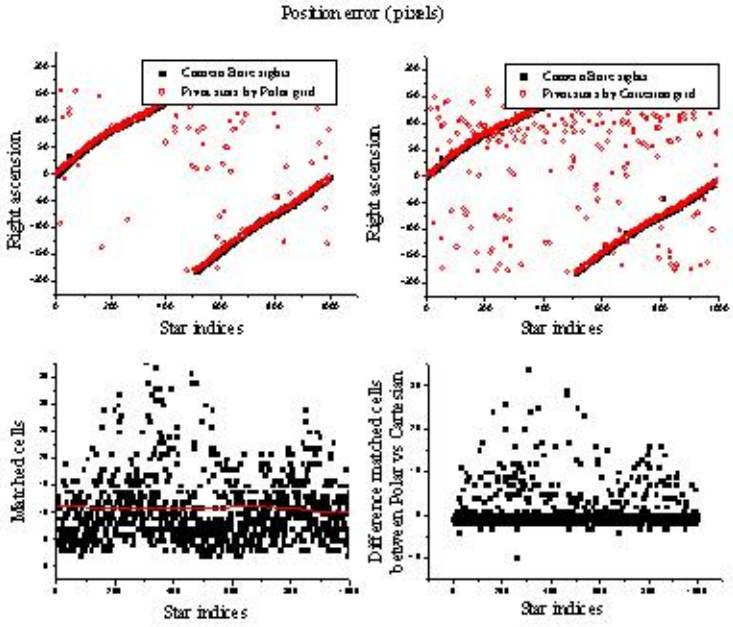

Fig.8 Comparison of Cartesian grid and Polar grid

The probability of star identification with position error of 2.5 pixels is about 0.98. Purely used grid algorithm without any modification methods excludes reference stars outside of the pattern radius. On the other hand, the grid algorithm using the virtual grid method uses the excluded reference stars by including it in the virtually generated grid. We can see that using all the reference stars imaged on the CCD with virtual grid. We can enhance the reliability of star identification.

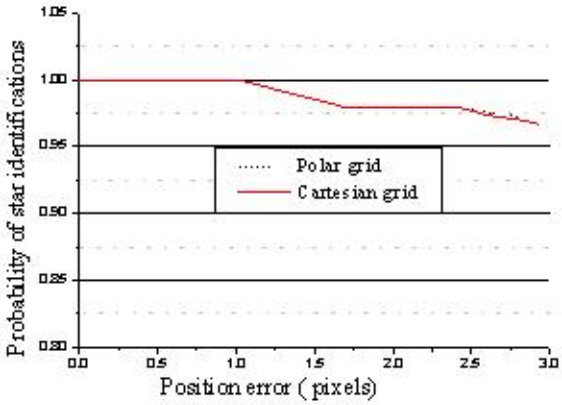

Fig.9 Probability of star identification by using virtual grid

Finally, multi-pivot selection method is applied to the polar coordinated grid algorithm. Multi-pivot selection method is activated only when there are less matched reference stars than threshold of minimum reference stars. We assume the following scenario for simulation. A spacecraft with a built-in star tracker is orbiting with sinusoidal motion shown as in Fig.10. To simulate the noisy environment, we applied 1.5 pixels position random Gaussian noise and 0.4 units apparent stellar magnitude random Gaussian noise. The overall identification rate for this scenario is over about 98.5%. The stars in the circle of Fig.10 come out as impossible images to be identified by the multi-pivot selection algorithm.

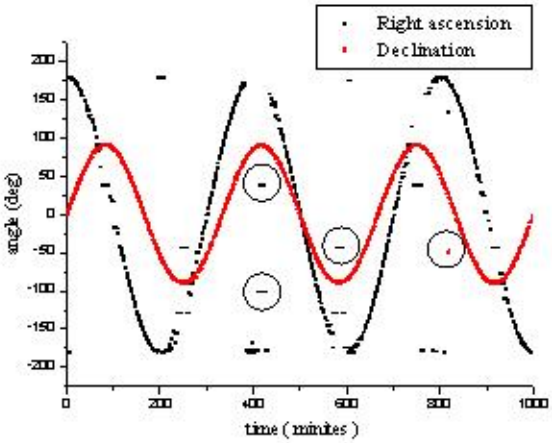

Fig.10 A scenario result by the proposed star identification

GROUND-BASED SYSTEMS

The star identification algorithms developed so far have been widely studied for many decades. However, literature for the ground test-bed system to demonstrate the proposed star identification algorithm is rare. In this section, the hardware development, setup, and tests are addressed. The developed ground-based system consists of three parts. One is pattern generation software, one other is star identification software, and the last one is the overall hardware system.

There may be two types of star pattern generation methods. One is for the reliable star tracker development for the space applications. These types of star pattern equipment generate star images could be same as the real star in space including various error sources. It could be hard not only to make the brightness same with the real star brightness in a laboratory, but also to construct the hardware system itself. The major drawback of the equipment is that the cost of the hardware system is very high.

Another type is for the test of star identification algorithms. Although the images are obtained in the real sky, most of the star identification algorithms use limited information. For example, most star identification methods don't need the information about the star brightness. The algorithm can effectively identify the stars without the brightness. Moreover, the brightness information in the CCD may be even not reliable. The equipment for the test of star identification algorithms is software based equipment. It could be implemented easily as well as constructed with low cost. In this paper, the star pattern generation software is developed.

The star pattern generation software is illustrated in Fig 11. The developed software has a variety of features. A major feature is to generate a star pattern for the given camera bore sight. Bright star catalog (BSC) is used in this software to generate the star pattern images. In the software it is assumed that there is a spacecraft orbiting the earth. The orbit of the spacecraft could be initially designed based on user demands. The user could also determine the direction cosine matrix of the star tracker with respect to the spacecraft body reference frame. Many of the initial parameters could be determined by using the initialization file of the software.

Some projection techniques should be used to display 3D positions of stars on 2D screen with limited distance, because the star positions with respect to the inertial frame are listed in the BSC based on right ascension and declination. The detail explanation about the projection techniques is not given here. To capture the reasonable star image using the CCD camera the alignment between the monitor displaying the 2D image and the CCD camera could be first accomplished. Calibration equipment is required to precisely accomplish the alignment of the two. To release the calibration burden, we added the calibration procedures into the star pattern generation software in stead of the calibration equipment. This procedure could prevent

the image of the CCD camera from distortion induced from the misalignment.

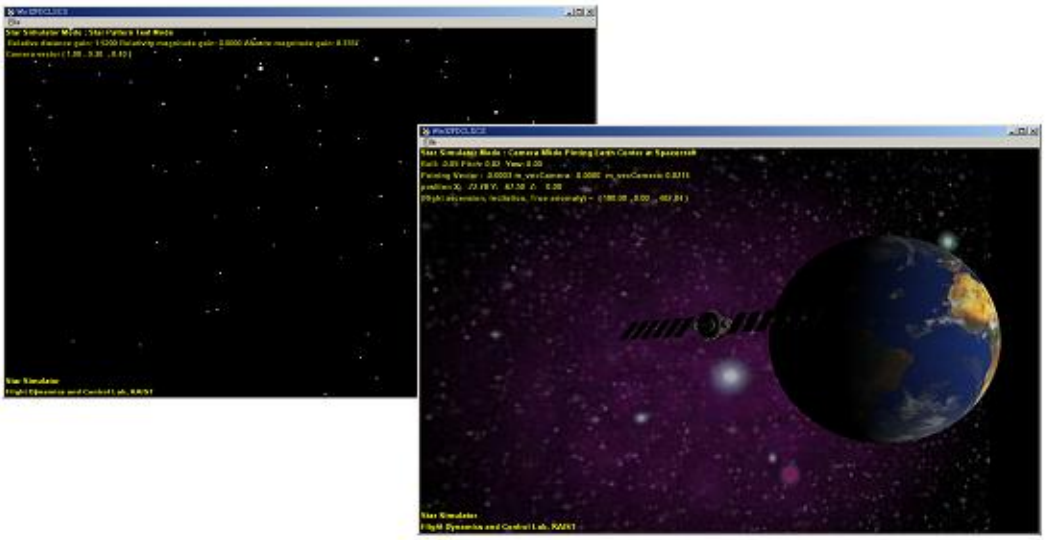

Fig.11 Star pattern generation software

Generally, the commercial CCD camera has an ability to adjust the field of view. The filed of view is directly related to the focal length. That is, it could be a hard work to focus the camera on the screen while satisfying the specific filed of view. Moreover, the star pattern software could also generate the identical star pattern of the CCD camera parameters. Most of these problems are resolved by adding various functions into the star pattern generation software.

To demonstrate the performance of the proposed algorithm by using the ground based system, an identification package for the star identification called star identification software is needed. The star identification software developed in this research is illustrated in Fig. 12. The implemented algorithm to identify the stars is based on the proposed polar grid method addressed in the previous section. Let us assume that the star pattern generation software produce certain images based on the specified CCD camera parameters. The star identification algorithm should be basically defined as the same CCD parameters. By doing that, the star identification package can surely identify the stars of the CCD image. To reduce such burdens as to perform the experiment the package also contains various functions. The initial parameters can be set by users using the GUI illustrated in the right side of Fig.12. There are two black screens. One of them is for the image to display of actually captured stars from CCD camera. Another is for the exact star pattern transferred from the star pattern generation software. The star identification software runs by pushing the start button. There is one more function optionally developed in the package. That function is to

control the attitude of hardware system using actuators. This option is closely depend on the hardware system.

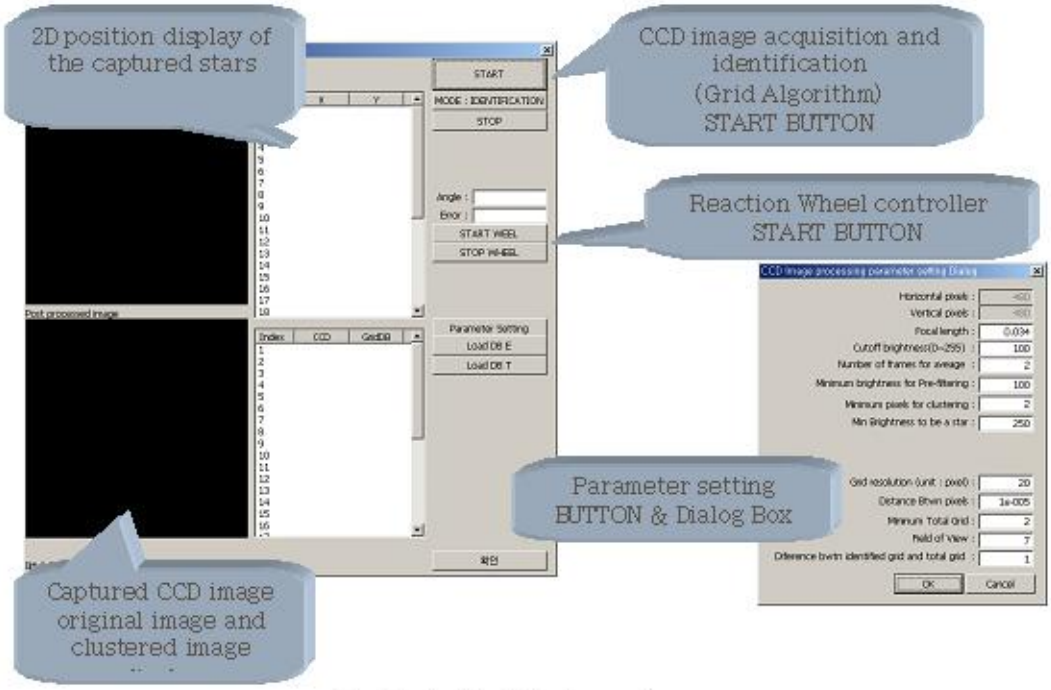

Fig.12 star identification software

The last one for the ground test of the proposed star identification algorithm is hardware system, which is illustrated in Fig. 13. The hardware system called 1 axis spacecraft H/W simulator consists of various sensors and actuators such as gyros, inertial measurement unit, reaction wheels and air thrusters. The large LCD monitor is used to display the star pattern produced by the star pattern generation software. The commercial CCD camera is utilized to a replacement of the star tracker. The camera is connected to the personal computer with an image capturing board installed in it. The captured images through the capturing board are transferred to the star identification software and displayed on the black screen of the software. Moreover, the hardware system has a capability to control 1-axis attitude by using the reaction wheels so that the optionally developed function of the star identification software could be utilized.

System setup to perform the ground test is firstly started by perpendicularly aligning the two parts : LCD monitor and the CCD camera. It is recommended to the camera direction vector is focus on the center of the LCD monitor to perform the experiment easily. Precise alignments are performed using the alignment functions of the star pattern generation software. By pushing the star button of the star identification software the ground test for the star identification is performed.

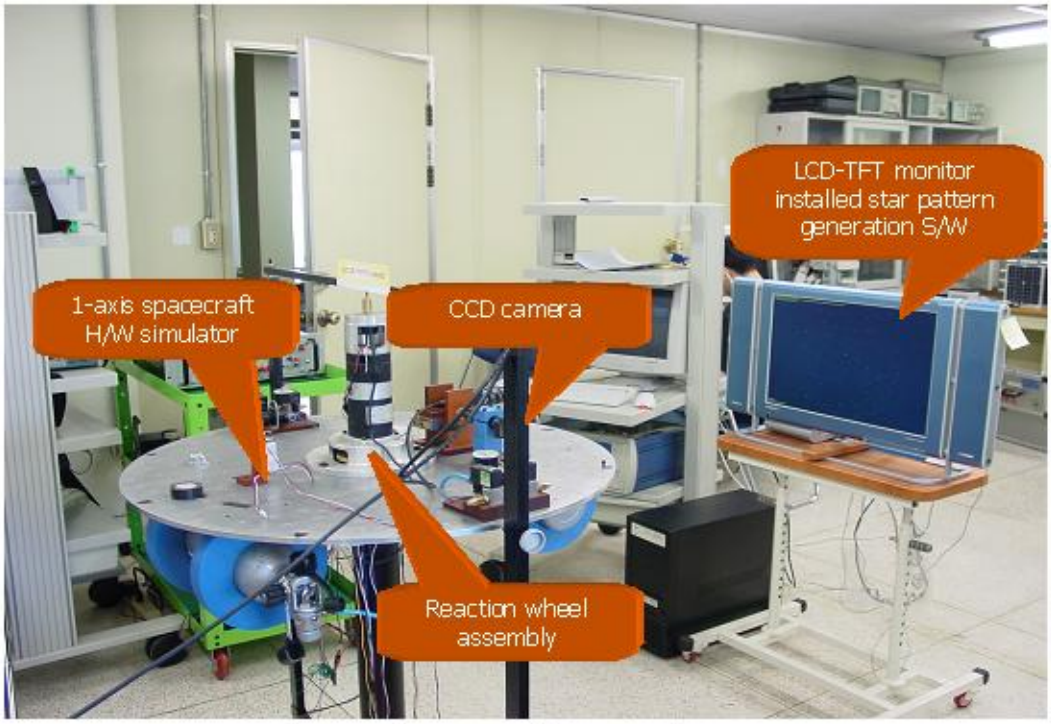

Fig.13 Hardware setup for star tracker tests.

The running time is about 600 sec to perform the experiment. The slewing rate of the simulated spacecraft to generate the star pattern in real-time is about 0.1deg/s. The slew rate is reasonable value to demonstrate the star tracker algorithm. The images captured from CCD camera in case of fast slew rate are not available to identify the stars so that fast image acquisition systems could be needed. Fig. 14 shows the trend of the pivot star vector from the captured images during the experiment. At first, the calibration process is performed during the first start time. The identified pivot stars near the center of the CCD image are plotted. There are some noisily cases near 500 sec. These cases are not the cases of fail to identify the stars. There could be two identified stars to be the pivot star far from the center of CCD image with similar distances. That is, the noisily cases could be explained by that the two stars are alternatively selected as a representative pivot star. By using the position vector of the pivot star with respect to the CCD frame, we can estimate the CCD camera vector. The estimated camera vector is illustrated in Fig.15. Classical QUEST or Least squares algorithm could be applicable to accurately estimate and determine the attitude using the identified stars. However, these estimation algorithms are out of scope in this paper so that the associated study is not given here. Consequently, we can conclude that the star identification using the proposed method in this paper is successfully achieved.

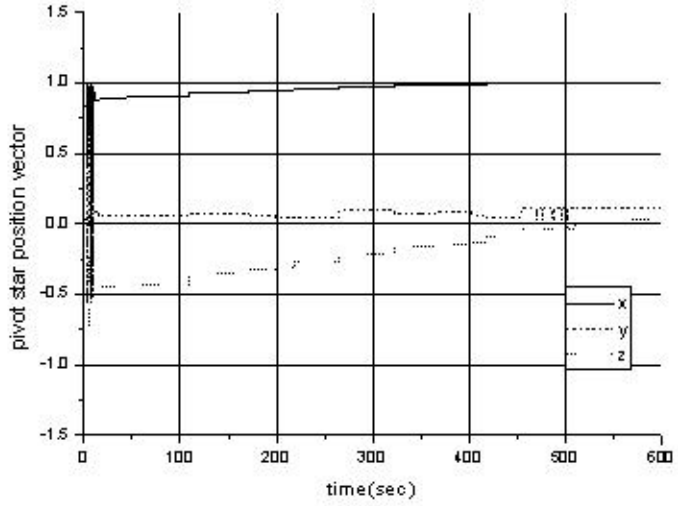

Fig.14 Trend of pivot star position vector.

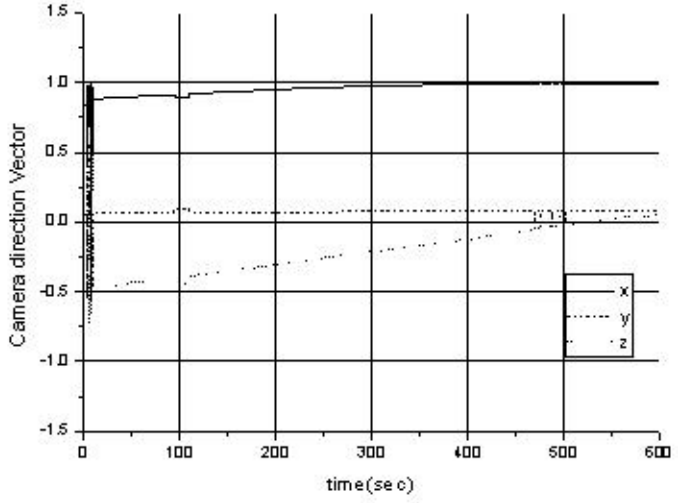

Fig.15 Trend of camera direction vector.

Attitude control could hardly be performed due to the attitude error accumulation while only using gyros. The attitude sensors such as star trackers are surely necessary to satisfactorily control the attitude of the spacecraft. The optionally developed attitude control function in the star identification package is also performed. For the attitude control experiment, the initial reference angle of the spacecraft H/W simulator is set to zero with

same as the initial output of the star tracker. The reaction wheel is used to perform the experiment. We can see from Fig. 16 that the experiment of the attitude control is successfully achieved. That is, the spacecraft H/W simulator is satisfactorily headed for the desired angle.

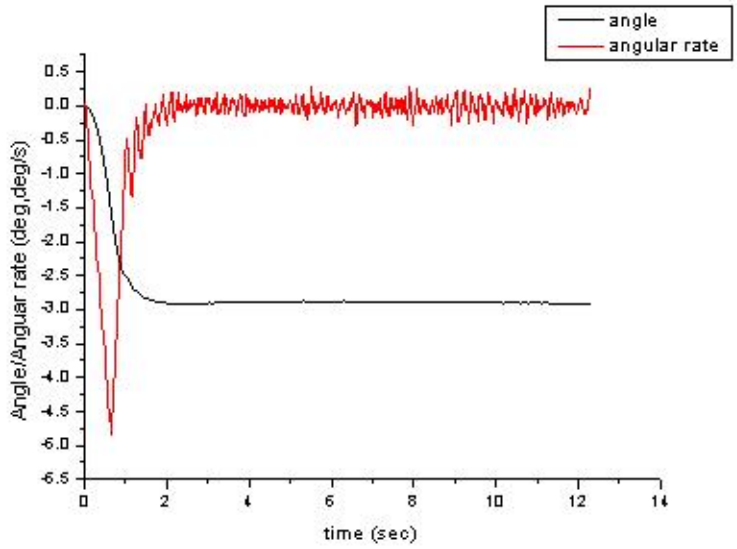

Fig.16 Responses of the angle and angular rate of the spacecraft H/W simulator.

CONCLUSIONS

A modified grid algorithm method is proposed. Proposed algorithm is demonstrated as an autonomous star identification algorithm about full celestial stars. The polar grid algorithm is proven as an autonomous method. The virtual grid is demonstrated that it plays very important role in star identification by enhancing star identification rates. Both the polar grid algorithm and Cartesian grid algorithm show enhanced star identification probability while using the virtual grid. The multi-pivot selection method is also a good reference to prevent mis-identification. We can anticipate a more reliable and autonomous star trackers by using the modified grid algorithm. To demonstrate the proposed algorithm within actual environment a ground test systems are developed. Finally, we could conclude that the proposed algorithm and the test system are successfully applicable to high performance star tracker developments.

REFERENCES

[1] J. L. Junkins, and C. C. White "Star Pattern recognition for real time attitude determination", *The Journal of the Astronautical Sciences*, 25, pp.251-270.

[2] C. C. Liebe, "Pattern Recognition of Star Constellations for Spacecraft Application," *IEEE Aerospace and Electrical Systems Magazine*, Vol.7, No.6, pp.10~16, 1992.

[3] F. Murtagh, "A New Approach to Point-pattern Matching," *Astronomical Society of Pacific*, Vol.104, pp.301~307.

[4] T. E. Strikwerda, and J. L. Junkins, "Star Pattern Recognition and Spacecraft Attitude Determination," Report ETL-0260, Engineering Topographic Lab.

[5] T. E. Strikwerda, H. L. Fisher, C. C. Kilgus, and L. J. Frank, "Autonomous Star Identification and Spacecraft Attitude Determination with CCD Stark Trackers," *Proceedings of the Conference on Spacecraft Guidance, Navigation and Control Systems*, 1991

[6] C.Padgett, K. Kreutz-Delgado, and S Udomkesmalee, "Evaluation of Star Identification Techniques," *Journal of Guidance, Control and Dynamics*. Vol.20, No.2, 1997, pp.259-267.